International Journal of Multiphase Flow 35 (2009) 801–810

Contents lists available at ScienceDirect

International Journal of Multiphase Flow

journal homepage: www.elsevier.com/locate/ijmulflow

Review

A scaling analysis for point–particle approaches to turbulent multiphase flows

S. Balachandar *

Department of Mechanical and Aerospace Engineering, University of Florida, 231 MAE-A, P.O. Box 116250, Gainesville, FL 32611, USA

ARTICLE INFO

Article history:
Received 11 June 2008
Accepted 10 February 2009
Available online 28 February 2009

Keywords:
Point-particle approach
Turbulence
DNS
LES

ABSTRACT

Simple dimensional arguments are used in establishing three different regimes of particle time scale, where explicit expression for particle Reynolds number and Stokes number are obtained as a function of nondimensional particle size (d/η) and density ratio. From a comparative analysis of the different computational approaches available for turbulent multiphase flows it is argued that the point–particle approach is uniquely suited to address turbulent multiphase flows where the Stokes number, defined as the ratio of particle time scale to Kolmogorov time scale (τ_p/τ_k), is greater than 1. The Stokes number estimate has been used to establish parameter range where point–particle approach is ideally suited. The point–particle approach can be extended to handle "finite-sized" particles whose diameter approach that of the smallest resolved eddies. However, new challenges arise in the implementation of Lagrangian–Eulerian coupling between the particles and the carrier phase. An approach where the inter-phase momentum and energy coupling can be separated into a deterministic and a stochastic contribution has been suggested.

1. Introduction

Point–particle approach has a long history (Riley and Paterson, 1974; Maxey, 1987; McLaughlin, 1989; Kallio and Reeks, 1989; Elghobashi, 1991) and more recently it has become a powerful and a useful tool in the computations of a variety of turbulent multiphase flows (Squires and Eaton, 1991; Elghobashi and Truesdell, 1992; Elghobashi and Truesdell, 1993; Wang and Maxey, 1993; Sundaram and Collins, 1997; Ferrante and Elghobashi, 2004). It is useful to think of a globally-undisturbed ambient flow that would exist in the absence of the particulate phase. A turbulent globally-undisturbed ambient flow is characterized by a range length and time scales from the Kolmogorov to the integral scale eddies. The disturbance flow generated around the particles has a range of scales and they are of the same order as the particles. The point–particle approach is on solid theoretical footing if the size of the suspended particles and the disturbance flow that they generate are much smaller than the scales of the undisturbed ambient flow. Note that at sufficient mass loading the back coupling of particles to the carrier phase becomes important and the energy spectrum of the carrier phase is modified from the undisturbed state.

In this scenario depicted in Fig. 1a the spectrum of scales generated around the particles and in their wakes can be considered microscale and it is well separated from the spectrum of the ambient carrier phase turbulence, which can be considered macroscale. This scale separation has been the basis of many point–particle Direct Numerical Simulations (DNS) (Riley and Paterson, 1974; Maxey, 1987; McLaughlin, 1989; Kallio and Reeks, 1989; Elghobashi, 1991; Squires and Eaton, 1991; Elghobashi and Truesdell, 1992; Elghobashi and Truesdell, 1993; Wang and Maxey, 1993; Sundaram and Collins, 1997; Ferrante and Elghobashi, 2004). These computations are DNS only at the macroscale. The microscale details of the flow at the scale of the particles are not directly computed, but taken into account in the simulations through inter-phase coupling models.

Often, it is not possible to computationally resolve the entire range of length and time scales even at the macroscale, and one needs to resort to Large Eddy Simulations (LES). Point–particle LES only requires that the particles are smaller than the smallest resolved scale and thus, particles can be substantially bigger than the Kolmogorov scale. This makes point–particle LES approach a very attractive tool for investigating high Reynolds number turbulent multiphase flows (Wang and Squires, 1997; Yamamoto et al., 2001).

In an overview of the point–particle approach, Elghobashi (1991, 1994) presented a regime map for the particle-laden turbulent flow. On a two parameter space of particle volume fraction (ϕ) and particle Stokes number (τ_p/τ_k – ratio of particle time scale to Kolmogorov time scale) he classified dilute and dense suspensions and provided guidelines for turbulence modulation. He compared the strengths and weaknesses of the two-fluid approach and the Lagrangian approach, both in the context of dilute and dense

* Tel.: +1 352 392 0961; fax: +1 352 392 7303.
E-mail address: bala1s@ufl.edu

0301-9322/$ - see front matter © 2009 Elsevier Ltd. All rights reserved.
doi:10.1016/j.ijmultiphaseflow.2009.02.013

suspensions. Here we follow this line of argument and consider in addition dusty gas and equilibrium Eulerian approaches (Ferry and Balachandar, 2001; Rani and Balachandar, 2003). Over the past decade fully resolved simulations of turbulent multiphase flows with $O(100)$ to $O(1000)$ particles and bubbles have also become possible (Pan and Banerjee, 1997; Kajishima et al., 2001; TenCate et al., 2004; Lu and Tryggvason, 2006; Uhlmann, 2008). In this paper we attempt to address the question, under what conditions and what range of parameters does point–particle DNS and LES approaches are ideally suited? Our discussion will however be limited to cases of dilute suspension and thus will avoid issues related to particle–particle interaction (four-way coupling). Towards this end, in Section 2 we first briefly review the different computational approaches available for turbulent multiphase flows. Then in Sections 3 and 4 we present simple dimensional arguments to establish scaling relations for relative particle velocity and particle Reynolds number. In Section 5 we establish the range of particle size and density ratio where point–particle DNS and LES approaches become the method of choice. Finally in Section 6 we discuss issues related to Lagrangian–Eulerian coupling between the particles and the carrier phase flow.

2. Point–particle vs other approaches

In general the term point–particle approach refers to Eulerian treatment of the carrier phase and Lagrangian treatment of the dispersed phase. A range of complementary computational approaches are available, each offering certain distinct advantages and disadvantages. A regime map for particle-laden turbulent flow with an insightful discussion on Eulerian (two-fluid) and Lagrangian approaches for the particles is presented in Elghobashi (1994).

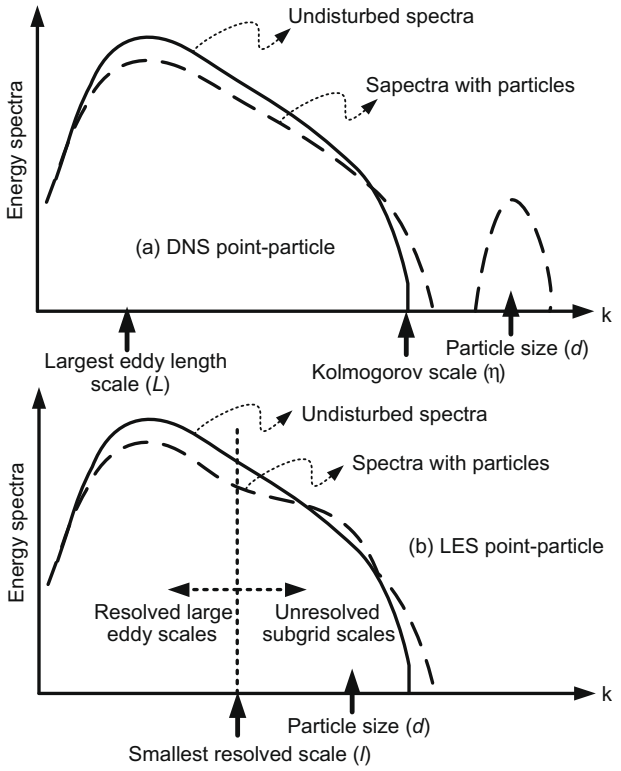

Fig. 1. Schematic of the energy spectra of the undisturbed flow and that of the particle-laden flow: (a) for the case of scale separation, when particles are much smaller than the undisturbed flow scales, (b) when there is no scale separation between the particle and the undisturbed flow.

Fig. 2 shows the different approaches and their applicability in the context of this map. The relative particle size (d/η, ratio of particle diameter to Kolmogorov scale) can be recast in terms of relative particle time scale or Stokes number (τ_p/τ_k). See Section 4 for a discussion on how nondimensional particle time and length scales are related. In discussing the spectrum of available approaches, each approach will be specifically compared with the prior approach and their relative advantages and disadvantages will be highlighted. Here we restrict attention to only dilute suspensions and thus issues pertaining to particle–particle interaction are avoided. Computational approaches, such as discrete element methods, that are appropriate to collision dominated flows will not be discussed.

2.1. Dusty gas approach

This powerful approach has been proposed and developed by Saffman, Marble and others (Saffman, 1962; Marble, 1970) in the context of particle-laden gas flows. In this approach it is assumed that the particles are sufficiently small that they perfectly follow the local carrier phase. In other words, in this limit the particle velocity is just the same as the surrounding fluid. This allows the particle-laden flow to be considered as a single fluid, whose density depends on the local mass fraction of suspended particles. The biggest advantage of this approach is its simplicity. In addition to mass, momentum and energy equations of the mixture only the concentration (or equivalently the number density) equation for the particulate phase needs to be solved. This approach is however applicable for only particles of very small time scale.

2.2. Equilibrium Eulerian approach

This approach can be thought of as the *Extended Dusty Gas Approach*, in the sense that it retains the computational simplicity and advantage of the dusty gas approach, but allows for particle velocity to be different from that of the surrounding carrier phase. In this approach it is assumed that the particles are sufficiently small that their motion is dictated only by the surrounding fluid. In other words, the particles are in equilibrium with the local carrier phase and their initial conditions have been forgotten. As shown in Ferry and Balachandar (2001) and Ferry et al. (2003) under equilibrium assumption particle velocity can be explicitly expressed as an expansion in terms of local fluid velocity and its gradients with the particle Stokes number (ratio of particle time scale to Kolmogorov scale) as the small parameter. For Stokes number less than unity even the first order correction to local fluid velocity provides accurate representation of the slip velocity between the particle and the surrounding fluid.

The biggest advantage over the dusty gas approximation is that the equilibrium Eulerian approach captures the relative particle motion much more accurately and thereby enable important phenomena, such as preferential particle accumulation (Squires and Eaton, 1991) and turbophoresis (Reeks, 1983), to be accounted for in the computation. A minor disadvantage over the dusty gas approach is that particle velocity cannot be simply taken to be that of local fluid, but it is given by an explicit algebraic equation involving local fluid velocity and its gradients. Simulations using this approach have been performed in turbulent flows (Ferry and Balachandar, 2002; Rani and Balachandar, 2003). Also, the equilibrium approach has been extended to express the temperature of the particle in terms of the local temperature of the fluid and its gradients (Ferry and Balachandar, 2005).

2.3. Eulerian approach

In this *two-fluid approach* both the carrier and the dispersed phases are treated as interpenetrating fluid media (Druzhinin

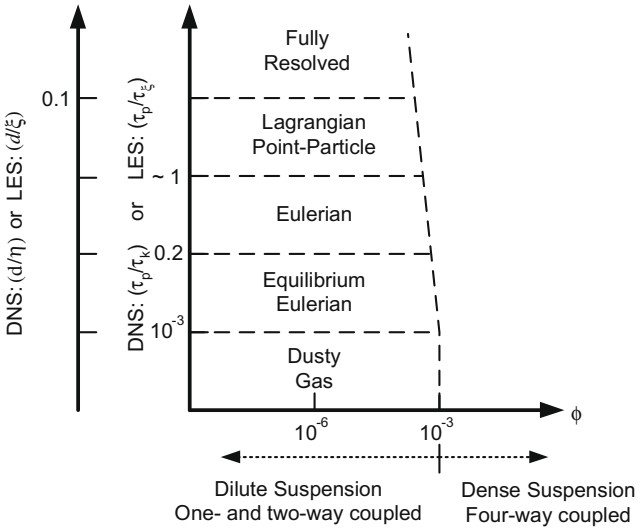

Fig. 2. The different approaches to turbulent multiphase flow. Their applicability is separated in terms of time scale ratio (Stokes number) or the length scale ratio, which are in turn related to each other.

and Elghobashi, 1999; Fevrier et al., 2005). As in the dusty gas and the equilibrium Eulerian approaches, the particulate phase is treated as a continuum and the particle velocity is given a field representation. While in the earlier two approaches only the momentum and energy equations of the carrier phase needs to be solved along with the concentration equation for the particulate phase, in the two-fluid formulation additional momentum and energy equations for the particulate phase must be solved with momentum and energy exchange between the phases taken into account as source and sink terms.

The advantage of the two-fluid formulation over the equilibrium approximation is that the restriction on particle Stokes number $(\tau_p/\tau_k < 1)$ can be somewhat relaxed. Thus, the Eulerian approach is applicable for particles that are larger than what could be accurately considered using the equilibrium approximation. Furthermore, there are situations when equilibrium assumption is clearly violated. For example, in cases where the particles are injected into the flow, even for particles of small Stokes number, there may be a region around the injector where particle velocity is controlled by the injection process. Only sufficiently away from the injector equilibrium will be applicable and the particle velocity can be accurately described in terms of local fluid velocity. Another instance of non-equilibrium is particle–shock interaction. In this case, there exists a region of relaxation downstream of the shock where the particle velocity adjusts to the post-shock gas velocity. Here again equilibrium approximation will be valid only sufficiently away from the shock.

The above advantages however come at a cost. In the standard Eulerian approach, for each particle size a set of mass, momentum and energy (partial differential) equations must be solved along with those of the carrier phase. While in the dusty gas and equilibrium Eulerian approaches only the mass (concentration) equation needs to be solved for the particles. Thus, the Eulerian approach is computationally expensive, and especially in the context of polydisperse systems, where a wide range of particle sizes need to be considered, the standard Eulerian approach can be very expensive. If the governing Eulerian equations are derived consistently using the PDF approach, one can include particle size as one of phase space variables. PDF based methods (Pope, 1985; Subramaniam, 2001; McGraw, 1997; Fox et al., 2008) have been advanced for numerical simulation of the resulting equations.

2.4. Lagrangian point–particle approach

In contrast to the different Eulerian descriptions of the dispersed phase described above, here we retain the true Lagrangian description of the particles by tracking their position, momentum and energy with their equations of motion. In the Eulerian approach we use field representations of particle properties, such as velocity and temperature, and this assumes existence of unique values of these properties. In other words, all particles within a tiny volume of fluid at any given point in space and time must have the same velocity, temperature, etc. This requirement of uniqueness in the Eulerian approach implicitly places restriction on the particle size and on the Stokes number that can be considered. Ferry and Balachandar (2001) showed that provided the particle time scale is less than the inverse of the maximal compressional strain-rate (their ratio can be thought of as a Stokes number) uniqueness can be guaranteed. If uniqueness is violated, then either a probabilistic framework must be adopted or the Eulerian fields of particle velocity, temperature, etc., must be thought of as ensemble averages. In the probabilistic framework, the phase space must be expanded beyond the space and time variables to include velocity and temperature information as well. Computations of turbulent multiphase flows using this probabilistic framework is impractical. Instead, if the Eulerian particle quantities represent ensemble averages, then the governing mass, momentum and energy equations for the particles will require closure assumptions.

Thus, the biggest advantage of the Lagrangian approach over any of the above Eulerian approaches is that there is no fundamental limitation on the particle time scale (or Stokes number), since there is no requirement of uniqueness. Furthermore, in the Lagrangian approach the size of each particle is independent and thus polydisperse systems can be handled easily, while in the Eulerian approaches, particle size spectrum must be partitioned into finite number of bins and the number of particles within each bin and their velocities and temperature must be treated with a set of field variables. On the other hand, coupling of the Lagrangian particles back to the carrier phase poses interesting challenges. Typically the hydrodynamic force on all the particles within a cell is added and distributed to the neighboring grid points. There needs to be sufficient number of particles within each cell in order to have a smooth Eulerian representation of the feed-back force from the particles. Since cell-to-cell fluctuation in the number of particles goes as inverse square root of the mean number of particles, even an average of 100 particles per cell gives rise to 10% fluctuation. With fewer number of particles per cell ad hoc smoothing of the feedback forcing is needed. Furthermore with fewer number of particles per cell, the algorithm by which the feed-back is apportioned to the neighboring cells is necessarily ad hoc and approximate. Thus, in the Lagrangian point–particle approach the computational cost increases, since a large number of particles must be tracked in order to contain the level of statistical fluctuation. Even when the computation employs on average a large number of particles, due to preferential accumulation, there are local regions of low particle number density adversely affecting accurate representation of local back coupling to the carrier phase. Also, as local number density decreases, the resulting increased grid-cell to grid-cell fluctuation poses serious problem in the evaluation of statistics of the dispersed phase. One other disadvantage of the Lagrangian approach is that it becomes exceedingly more expensive, due to restriction in time step size, as the particle size decreases, e.g. in reacting flow applications with evaporating droplets.

2.5. Fully-resolved approach

All the above methods, either explicitly or implicitly, make the point–particle approximation, and thus are restricted to particles

of size much smaller than the Kolmogorov scales, or the smallest resolved eddies in case of LES. The point–particle assumption is clear in the context of Lagrangian approach. In the context of the Eulerian approaches the force and heat transfer laws that are used to account for the momentum and energy coupling between the phases are invariably based on the assumption that the particles are much smaller than the flow scales.

For particles of size comparable or larger than the smallest undisturbed flow scales the ultimate option is to perform fully resolved DNS, where all the scales of ambient turbulence, and the flow scales introduced by the particles (the unsteady boundary layers and the wakes) are completely resolved. Such simulations have been performed for a single particle (Bagchi and Balachandar, 2003; Bagchi and Balachandar, 2004; Merle et al., 2005; Burton and Eaton, 2005; Zeng et al., 2008) to a collection of up to $O(100)$ particles in turbulent flows (Pan and Banerjee, 1997; Kajishima et al., 2001; TenCate et al., 2004; Lu and Tryggvason, 2006; Uhlmann, 2008). Most applications typically involve far more particles in the flow than few thousand, and fully-resolved DNS of such systems is out of question in the foreseeable future.

3. Relative velocity

3.1. General analysis

Here we obtain a simple estimate of the relative velocity between the particle and the surrounding fluid in a turbulent flow. A preliminary discussion along this line was presented in an earlier paper (Balachandar, 2003). Let L and η denote the largest (integral) and the smallest (Kolmogorov) scales of the turbulent flow and d be the diameter of the particles. The corresponding time and velocity scales of the L-size eddies are given by $\tau_L = L^{2/3}/\epsilon^{1/3}$ and $u_L = (\epsilon L)^{1/3}$ and those of the Kolmogorov eddies are given by $\tau_k = \eta^{2/3}/\epsilon^{1/3}$ and $u_k = (\epsilon\eta)^{1/3}$, where ϵ is the dissipation rate that is considered to be set by the energy containing large eddies and maintained through the inertial range. The particle time scale is given by

$$\tau_p = \frac{(2\rho+1)}{36}\frac{d^2}{\nu}\frac{1}{\phi(\mathrm{Re})}, \tag{1}$$

where ν is the kinematic viscosity of the surrounding fluid, $\rho = \rho_p/\rho_f$ is the particle-to-fluid density ratio and ϕ is the finite Reynolds number correction to Stokes drag, which for solid particles can be taken to be $\phi(\mathrm{Re}) = 1 + 0.15\mathrm{Re}^{0.687}$ (Clift et al., 1978). Similar finite Reynolds number corrections for bubbles has been presented by Mei (1994). Here the Reynolds number is based on particle diameter and the relative velocity between the particle and the surrounding fluid: $\mathrm{Re} = |u - v|\, d/\nu$.

In the context of DNS of the carrier phase turbulence, as discussed above, we are limited to small particles that satisfy $L \gg \eta \gg d$. In estimating the relative velocity we make use of the equilibrium Eulerian approximation for the particle velocity (Ferry and Balachandar, 2001; Ferry et al., 2003) as given by $(u - v) \approx \tau_p(1-\beta)Du/Dt$, where $\beta = 3/(2\rho+1)$ is a parameter associated with density ratio and Du/Dt is fluid acceleration seen by the particle. Note β is bounded to be $O(1)$, with $\beta = 0$ for heavy particles, $\beta = 1$ for neutrally buoyant particles and $\beta = 3$ for bubbles. As discussed in (Ferry and Balachandar, 2001; Ferry et al., 2003) a simple interpretation for the above relation is that under equilibrium particle motion the relative velocity is dictated by particle's inability to respond to local fluid acceleration just as a fluid element. It must be stressed that here equilibrium does not imply that the particles move with the fluid. It implies that the particle velocity depends only on the surrounding fluid and that the effects of particle's initial conditions have decayed rapidly. As a result, in an accelerating flow a heavy particle ($\beta = 0$) will lag the fluid, while a bubble ($\beta = 3$) will lead the fluid.

The total acceleration derives contributions from the entire spectrum of eddies and that due to the l-size eddy can be estimated from the inertial scaling as $(Du/Dt)_l = u_l/\tau_l$, where $u_l = (\epsilon l)^{1/3}$ and $\tau_l = l^{2/3}/\epsilon^{1/3}$. By substituting in the equilibrium Eulerian approximation for the relative velocity it can be see that the relative velocity induced by the l-size eddy can be expressed as

$$\frac{(u-v)_l}{u_l} \approx \begin{cases} (1-\beta)\frac{\tau_p}{\tau_l} & \text{if } \tau_p < \tau_l, \\ (1-\beta) & \text{if } \tau_p > \tau_l. \end{cases} \tag{2}$$

In the above it is assumed that for small particles the relative velocity due to the l-size eddy increases with τ_p as given by the equilibrium approximation. However, for larger particles of time scale greater than τ_l relative velocity will be capped at $(1-\beta)u_l$ (note equilibrium approximation is accurate only for $\tau_p/\tau_l < 1$). The above simplified model is sufficient for the present discussion. A slightly improved approximation is presented in the Appendix.

3.2. Three different regimes

For each particle size (and corresponding particle time scale), the relative velocity due to the different eddies from the Kolmogorov to the integral scale can be estimated and the largest contribution can be taken to be the characteristic relative velocity for the particle. In doing so, three different regimes of particle size can be identified:

(1) In regime-I particles are sufficiently small that their time scale is smaller than the Kolmogorov time scale. Since the time scale of eddies increases as two-third power of eddy size, the time scale of particles in regime-I is guaranteed to be less than all carrier flow time scales. It can be readily obtained that in regime-I the relative velocity of particles is controlled by the Kolmogorov eddies and we have

$$\underline{\mathrm{Regime-I}}\ (\tau_p < \tau_k): \qquad \frac{(u-v)}{u_k} \approx \frac{\tau_p}{\tau_k}(1-\beta). \tag{3}$$

The above estimate of relative velocity can be rearranged to obtain

$$\frac{(u-v)}{u_k} \approx \frac{(2\rho+1)}{36}\frac{(1-\beta)}{\phi(\mathrm{Re})}\left(\frac{d}{\eta}\right)^2. \tag{4}$$

It will be shown below that particle Reynolds number in regime-I is constrained to be small and Stokes drag applies (i.e., $\phi \approx 1$). The dependence of relative velocity on density ratio and relative particle size becomes clear.

(2) Regime-II is comprised of larger particles, whose time scale exceeds the Kolmogorov time scale, but is less than τ_L. For particles in this regime, there exist an eddy of size $l_* = \tau_p^{3/2}\epsilon^{1/2}$, which satisfies the condition $\eta < l_* < L$, whose time scale matches the particle time scale. Such particles are too big to fully respond to eddies of size smaller than l_* and the maximum relative velocity will be dictated by the l_*-size eddy, i.e., $(u-v)_{l_*} \approx (1-\beta)(\epsilon l_*)^{1/3} = (1-\beta)(\epsilon\tau_p)^{1/2}$. Now consider the effect of eddies of size $l_1 > l_*$. Since their time scale is larger than that of the particle, the relative velocity due to an eddy of size l_1 can be estimated using the equilibrium Eulerian approximation as $\tau_p(1-\beta)(Du/Dt)_{l_1} \approx \tau_p(1-\beta)\epsilon^{2/3}/l_1^{1/3}$. The ratio of estimated relative velocity due to the l_1-eddy and the smaller l_*-eddy is given by

$$\tau_p\frac{\epsilon^{2/3}}{l_1^{1/3}}\frac{1}{(\epsilon\tau_p)^{1/2}} = \left(\frac{l_*}{l_1}\right)^{1/3} < 1. \tag{5}$$

It is thus established that

$$\underline{\mathrm{Regime-II}}\ (\tau_k < \tau_p < \tau_L): \quad (u-v) \approx (1-\beta)(\epsilon\tau_p)^{1/2} \quad \Rightarrow \quad \frac{(u-v)}{u_k} \approx (1-\beta)\left(\frac{\tau_p}{\tau_k}\right)^{1/2}. \tag{6}$$

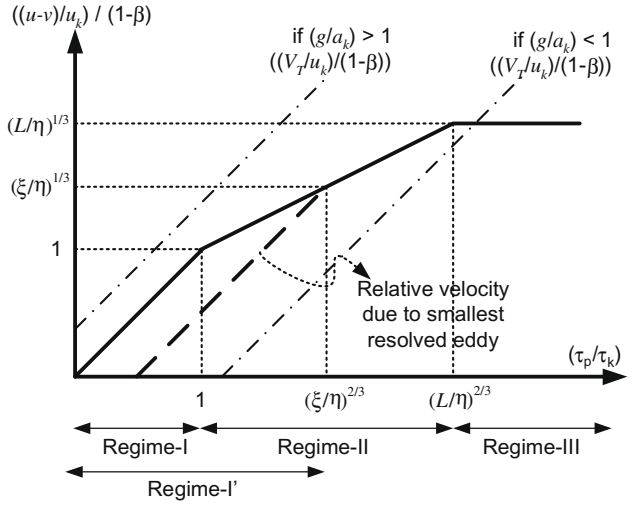

Fig. 3. Log–log plot of nondimensional relative velocity against particle Stokes number. The three solid line segments show the relative velocity in the three different regimes and their boundaries are marked as well. The dashed line captures the relative velocity due to the resolved scales in case of LES. The dash–dot lines show relative settling velocity, $(V_T/u_k)/(1-\beta)$ plotted against τ_p/τ_k for are two possible scenarios of acceleration due to gravity. If $g/a_k > 1$ then relative velocity dues to settling dominates and if $g/a_k < 1$ then for small τ_p/τ_k turbulence effects dominate relative velocity, but for larger particles gravity effect will dominate.

(3) Similar arguments can used for regime-III particles, whose time scale exceeds the time scale of the largest eddy (τ_L). The relative velocity for the regime-III particles is capped by the velocity scale of the L-sized eddies. The relative velocity is then given by

$$\underline{\text{Regime} - \text{III}}\ (\tau_L < \tau_p): \quad (u-v) \approx (1-\beta)(\epsilon L)^{1/3} \quad \Rightarrow \quad \frac{(u-v)}{u_k} \approx (1-\beta)\left(\frac{L}{\eta}\right)^{1/3}. \tag{7}$$

The relative velocity normalized by the Kolmogorov velocity $((u-v)/u_k)$ in the three regimes are plotted as a function of τ_p/τ_k in Fig. 3, and the different power-law behaviors in the different regimes are clear. Note that in the above estimation, equilibrium velocity is employed only for sufficiently small particles whose time scale is smaller than the eddy. For larger particles relative velocity is capped by the velocity scale of the eddy, which is given by turbulence scaling.

3.3. Relative velocity scaling in LES

We can now investigate the relative velocity scaling in the context of LES of carrier phase turbulence. Let $\xi > \eta$ be the cut-off length scale. Only eddies of size larger than the cut-off are computed in LES and scales below the cut-off are considered subgrid and as a result modeled. The arguments presented above in the context of DNS of carrier phase can be extended to the case of LES as well. However, the smallest resolved length scale (ξ) now plays a role similar to the role Kolmogorov scale (η) played in the above analysis. We can identify regime-I′ where the particle time scale is less than the time scale of the smallest resolved eddy ($\tau_\xi = \xi^{2/3}/\epsilon^{1/3}$). In this regime the relative velocity is dictated by the smallest resolved eddy and is given by

$$\underline{\text{LES Regime} - \text{I}'}\ (\tau_p < \tau_\xi): \quad \frac{(u-v)}{u_k} \approx (1-\beta)\frac{\tau_p}{\tau_k}\left(\frac{\eta}{\xi}\right)^{1/3}. \tag{8}$$

This regime, which is relevant to LES, is also depicted in Fig. 3 and as can be expected it covers all of DNS regime-I and part of regime-II. In this LES regime-I′ the relative velocity induced by the resolved eddies is smaller than what can be expected with the presence of the subgrid scales. For particles whose time scale is larger than τ_ξ, the dominant eddy which controls the relative velocity is being computed as part of LES and as a result the relative velocity scaling remains the same as in DNS (same as given in Eqs. (6) and (7)).

In LES, in computing the Lagrangian motion of particles, in addition to the resolved scale carrier flow velocity seen by the particle, a stochastic component that accounts for the effect of the unresolved subgrid scales is also included (Minier et al., 2004; Shotorban and Mashayek, 2006; Berrouk et al., 2007). If appropriately accounted, the effect of the subgrid should bring the relative velocity scaling back to the DNS level and as a result the estimates of relative velocity given in (3), (6) and (7) are applicable even in LES. The important difference is that the stringent point–particle DNS requirement that $d \ll \eta$ is relaxed and replaced by $d \ll \xi$. The above discussion clarifies the role of stochastic contribution to the particle motion. For small particles of time scale less than τ_ξ the stochastic contribution will dominate and dictate the magnitude of relative velocity. Whereas for larger particles the stochastic contribution to relative velocity will be sub-dominant to the deterministic contribution arising from the resolved scale eddies. Nevertheless, for all particles the stochastic contribution is important in order to properly account for the role of subgrid scales in particle dispersion.

3.4. Role of settling velocity

In the above discussion the effect of gravity and particle settling has not been factored. Particle settling velocity (V_T) is linearly related to particle time scale as $V_T = \tau_p g(1-\beta)$, where g is acceleration due to gravity. From which nondimensional particle settling velocity can be obtained as

$$\frac{V_T}{u_k} = \frac{\tau_p}{\tau_k}(1-\beta)\frac{g}{a_k}, \tag{9}$$

where $a_k = \epsilon^{2/3}/\eta^{1/3}$ is Kolmogorov acceleration. The two different situations of (g/a_k) being greater than one and less than one are depicted in Fig. 3. It can be seen that provided $(g/a_k) > 1$ gravitational settling will dictate the relative velocity of all particles. On the other hand, if $(g/a_k) < 1$ for a range of small particle size their settling velocity will be smaller than relative velocity induced by the turbulent eddies. But there exist a particle size (or equivalently a particle time scale) beyond which settling velocity will exceed relative velocity due to turbulence.

A more quantitative estimate can be obtained with the following definition of Kolmogorov acceleration in terms of kinematic viscosity of the fluid: $a_k = \nu^2/\eta^3$. Consider the following typical cases. In water at around room temperature ($\nu \approx 10^{-6}$ m^2/s), if Kolmogorov scale $\eta > 47$ μm, then in such turbulence gravitational settling will dominate the effect of turbulent eddies in determining relative velocity. The above result is independent of particle-to-fluid density ratio and therefore is applicable for both bubbles and heavy suspended particles. In air at around room temperature ($\nu \approx 1.5 \times 10^{-5}$) provided $\eta > 284$μm gravitational settling will always dictate relative velocity. Note that in all these cases the importance of gravitational settling compared to turbulence is determined by the Kolmogorov scale and is independent of the Reynolds number of the carrier phase turbulence.

4. Particle Reynolds number

Here we use the relative velocity scaling obtained in the previous section to obtain the particle Reynolds number scaling. Again

the three different regimes are of relevance. The relative velocity in the different regimes (Eqs. (3), (6), and (7)) can be used to obtain equations for particle Reynolds number and after algebraic manipulation we get

$$\mathrm{Re}\phi(\mathrm{Re}) = \frac{|\rho-1|}{18}\left(\frac{d}{\eta}\right)^3 \quad \text{Regime-I} \tag{10}$$

$$\mathrm{Re}\sqrt{\phi(\mathrm{Re})} = \sqrt{\frac{1}{2\rho+1}}\frac{|\rho-1|}{3}\left(\frac{d}{\eta}\right)^2 \quad \text{Regime-II} \tag{11}$$

$$\mathrm{Re} = \frac{2|\rho-1|}{2\rho+1}\frac{d}{\eta}\left(\frac{L}{\eta}\right)^{1/3} \quad \text{Regime-III.} \tag{12}$$

The domain of validity of the three regimes can now be recasted entirely in terms of particle-to-fluid density ratio and nondimensional particle diameter. In order to do so first we combine (10) with the boundary between regime-I and regime-II (i.e., $\tau_p = \tau_k$) to obtain

$$\mathrm{Re}_{\mathrm{I,II}} = \frac{2|\rho-1|}{2\rho+1}\frac{d}{\eta}. \tag{13}$$

This indicates that particle Reynolds number in regime-I is much smaller than unity. Similarly, we can combine (11) with $\tau_p = \tau_L$ to obtain the following Reynolds number for the boundary between regime-II and regime-III

$$\mathrm{Re}_{\mathrm{II,III}} = \sqrt{\frac{2|\rho-1|}{2\rho+1}}\frac{d}{\eta}\left(\frac{L}{\eta}\right)^{1/3}. \tag{14}$$

Using the above relations the three different regimes can be uniquely defined in terms of ρ and d/η as

$$\text{Regime-I}: \left(\frac{2\rho+1}{36}\right)\left(\frac{d}{\eta}\right)^2 < \phi(\mathrm{Re}_{\mathrm{I,II}}) \tag{15}$$

$$\text{Regime-II}: \phi(\mathrm{Re}_{\mathrm{I,II}}) < \left(\frac{2\rho+1}{36}\right)\left(\frac{d}{\eta}\right)^2 < \phi(\mathrm{Re}_{\mathrm{II,III}})\left(\frac{L}{\eta}\right)^{2/3} \tag{16}$$

$$\text{Regime-III}: \phi(\mathrm{Re}_{\mathrm{II,III}})\left(\frac{L}{\eta}\right)^{2/3} < \left(\frac{2\rho+1}{36}\right)\left(\frac{d}{\eta}\right)^2. \tag{17}$$

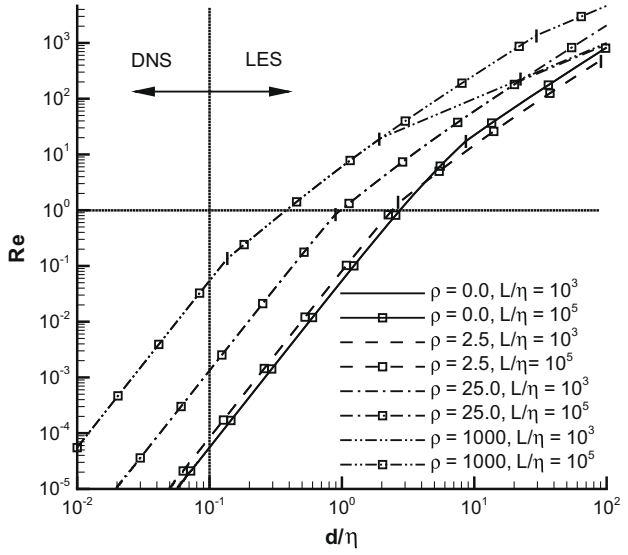

Fig. 4. The plot of particle Reynolds number vs nondimensional particle size, for varying density ratio and turbulence intensity given in terms of ratio of integral to Kolmogorov length scale. In each plot the boundary between the different regimes is marked by a vertical bar.

Note that in DNS point–particle approach $\mathrm{Re}_{\mathrm{I,II}}$ will be less than one and as a result we have the approximation $\phi(\mathrm{Re}_{\mathrm{I,II}}) \approx 1$. In the context of LES, however, the particle diameter can exceed the Kolmogorov scale and the regime boundaries must be obtained corresponding to finite Re.

Fig. 4 presents Reynolds number plotted as a function of d/η for different values of density ratio and carrier phase turbulence Reynolds number. Note that $L/\eta = (\mathrm{Re}_L)^{3/4}$ and the ratio of integral to Kolmogorov length scale is related to turbulence Reynolds number. Under equilibrium assumption neutrally buoyant particles ($\rho = 1$) move with the fluid and as a result their relative velocity and Reynolds number are zero. From (10) it can be seen that in regime-I the Reynolds number of $\rho = 2$ particles and $\rho = 0$ bubbles is the same. In regime-II Eq. (11) shows that the Reynolds number of $\rho = 4$ particles is the same as that of bubbles. In regime-III according to (12) the Reynolds number of bubbles will be the largest and larger than even the heaviest particles. These behaviors can be verified in Fig. 4. In regime-I the Reynolds number of $\rho = 2.5$ particles is slightly higher than that of bubbles, while in regime-II the trend reverses. In both these regimes with further increase in density ratio particle Reynolds number substantially increases.

If we restrict to $d/\eta < 0.1$ then particle Reynolds number remains quite small even for very heavy particles. In case of large density ratio ($\rho \approx 1000$) as d approaches Kolmogorov scale, particle Reynolds number increases above 1. In case of bubbles only in the context of LES, as the particle diameter increases substantially above the Kolmogorov scale, Re increase above 1. In Fig. 4 the boundary between the different regimes is marked by vertical bars. Bubbles and $\rho = 2.5$ particles, even as large as $d \approx 100\eta$, are still in regime-II. Over the range of d/η shown in Fig. 4 only the heavy particles have entered regime-III. In regimes-I and II particle Reynolds number is independent of turbulence intensity (or L/η). Only in regime-III Re depends on L/η and as can be expected with increasing turbulence intensity particle Reynolds number increases.

5. Point–particle approach – method of choice

From the comparison of the different approaches presented in Section 2 it can be argued that the point–particle Lagrangian approach is uniquely suited in problems where the particle time scale is larger than the Kolmogorov time scale (i.e., $\tau_p/\tau_k > 1$). The point–particle approach is clearly applicable even when $\tau_p/\tau_k < 1$, however, when this ratio (Stokes number) is small the equilibrium Eulerian approach offers a more computationally efficient alternative. The accuracy of the equilibrium approximation has been tested in a variety of turbulent flows and it appears that provided the Stokes number (τ_p/τ_k) is less than about 0.2 fairly accurate results are obtained with the equilibrium Eulerian approach (Ferry and Balachandar, 2002; Rani and Balachandar, 2003; Shotorban and Balachandar, 2006). In the limit $\tau_p/\tau_k \ll 1$ one may even simply use the dusty gas approximation. For the case $0.2 < \tau_p/\tau_k \sim O(1)$ both the Eulerian two-fluid formulation and the Lagrangian point–particle approach become comparable. For larger particles of $\tau_p/\tau_k > 1$, since uniqueness of particle velocity cannot be guaranteed, the Lagrangian approach offers an advantage.

The point–particle approach is on sound theoretical footing in the limit $d \ll \eta$. However, in problems involving millions of particles of size comparable to the Kolmogorov scale, the point–particle approach may be the only viable option provided $\tau_p/\tau_k > 1$, since a fully-resolved simulation is not an option. The point–particle approach in such cases where the particles are comparable to the Kolmogorov scale can be appropriately termed "finite-size point–particle approach". As will be seen below inter-phase momentum

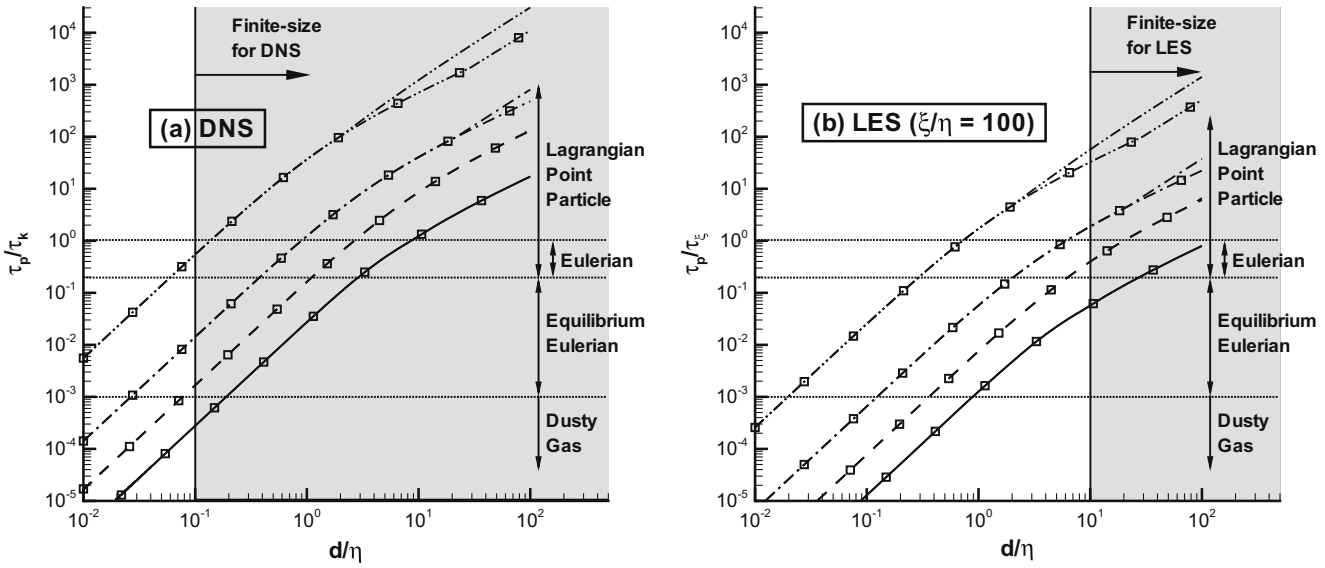

Fig. 5. The plot of time scale ratio vs nondimensional particle size, for varying density ratio and turbulence intensity given in terms of ratio of integral to Kolmogorov length scale. (a) τ_p/τ_k plotted for DNS of carrier phase; (b) τ_p/τ_l plotted for LES of carrier phase with the assumption that the ratio of cut-off length scale to Kolmogorov scale is 100. The legends for the different lines and symbols are the same as in Fig. 4. In both cases it is arbitrarily assumed that particles of diameter greater than 0.1 times the smallest eddy size will be considered big.

and energy coupling becomes complicated as the particle size increases and approaches the Kolmogorov scale and unavoidable empiricism needs to be introduced in their representation. Nevertheless, from (1) it can be seen that

$$\frac{\tau_p}{\tau_k} = \frac{2\rho+1}{36}\frac{1}{\phi(Re)}\left(\frac{d}{\eta}\right)^2. \tag{18}$$

The particle Reynolds number dependence obtained in Section 4 can now be used to express the Stokes number entirely in terms of d/η and density ratio. In Fig. 5a τ_p/τ_k is plotted against d/η on log–log scale for different combinations of ρ and L/η. If we restrict attention to $d/\eta < 0.1$, even for the case of heavy particles in gas ($\rho \sim O(10^3)$), the time scale ratio is generally small and the point–particle Lagrangian approach is barely the method of choice. However, if we relax the particle size restriction and consider $d \sim O(\eta)$, then for heavier-than-fluid particles the time scale ratio can increase above unity and point–particle approach becomes more appropriate. The above analysis is pertinent to the case of DNS of carrier phase. From Fig. 4 it can be seen that for small values of d/η particle Reynolds number is generally small. Accordingly $\phi(\mathrm{Re}) \sim 1$ and as a result the time scale ratio simply shows a quadratic dependence on d/η.

In case of LES of carrier phase, the point–particle approach becomes the method of choice provided the particle time scale is larger than the time scale of the smallest resolved eddy (i.e., $\tau_p > \tau_\xi$). The time scale ratio can now be expressed as

$$\frac{\tau_p}{\tau_\xi} = \frac{2\rho+1}{36}\frac{1}{\phi(Re)}\left(\frac{d}{\xi}\right)^2\left(\frac{\xi}{\eta}\right)^{4/3}. \tag{19}$$

In Fig. 5b τ_p/τ_ξ is plotted against d/η on log–log scale for different combinations of ρ and L/η, for the particular case where the LES filter is 100 times the Kolmogorov scale. Thus, even if we limit to particle size an order of magnitude smaller than the smallest resolved eddy (i.e., $d/\xi \sim 0.1$), provided the Reynolds number of carrier phase turbulence is sufficiently large and accordingly the cut-off length scale much larger than Kolmogorov scale ($\xi/\eta \gg 1$), the time scale ratio can be greater than 1 for a wide range of density ratio to make point–particle approach the method of choice. Again point–particle LES approach can be pushed to consider larger particles of size comparable to the filter size (i.e., $d \sim \xi$). In which case even for bubbly flows ($\rho \to 0$) the Lagrangian point–particle approach may be the only viable option. Note that in Fig. 5, even for the $\rho = 0$ bubble case, the finite Re correction applied is corresponding to that of rigid sphere. Instead $\phi(\mathrm{Re})$ proposed by Mei (1994) for bubbles can be used, but the corresponding change is minor.

6. Inter-phase coupling

6.1. Point–particle DNS

Momentum coupling between the phases is enforced in terms of drag and lift forces between the individual particles and the surrounding fluid. These forces that act on the particles are used in solving the Lagrangian equations of motion. The forces are also back coupled to the carrier phase momentum equation. Although this sounds simple enough, there are subtle issues that complicate this Eulerian–Lagrangian coupling between phases.

If the Reynolds number, based on particle diameter and relative velocity with the ambient flow, is sufficiently small, reliable analytical expressions for drag and lift forces exist (Clift et al., 1978). At finite Reynolds numbers the drag and lift forces are given by empirical correlations. Furthermore, additional forces such as added-mass, Bassett history and Faxen correction can become important for finite-sized particles. Irrespective, the analytical expressions and empirical correlations are in terms of the undisturbed ambient carrier phase. For example, the standard drag correlation is given in terms of the undisturbed carrier phase velocity as seen by the particle. Undisturbed carrier phase velocity for each particle technically requires the knowledge of the flow that would have existed in its absence. Note that in this sense the undisturbed carrier phase velocity for each particle is different from the globally-undisturbed velocity discussed at the very beginning in the introduction. While the globally-undisturbed velocity is a single

phase flow, local undisturbed flow for each particle will include the effect of all far away particles. Nevertheless, as long as the particle and the disturbance flow it locally generates are substantially smaller than the Kolmogorov scale, the separation of undisturbed and disturbance flows at the macro and microscale is feasible (see Fig. 1a). And the undisturbed fluid velocity seen by the particle can be taken to be the carrier phase velocity at the grid scale. Furthermore, for such small particles, the effect of undisturbed flow gradients at the macroscale will be substantially weak and the force on the particle can be reliably taken to be given by the standard drag correlation.

The above considerations equally apply to thermal energy exchange between the particles and the carrier phase. For sufficiently small particles, energy exchange can be accurately predicted using standard heat transfer correlations, where again the temperature of the undisturbed ambient fluid can be taken to be the carrier phase temperature at the grid scale.

As the particles approach the scales of the undisturbed flow, there will not be any scale separation between the macroscale turbulence and the microscale flow features around the particles. The energy spectra is illustrated by the dash line in Fig. 1b. This situation significantly complicates the momentum and energy exchange between the particles and the carrier phase that enters in the governing equations as inter-phase force and heat transfer terms. As we extend the point–particle approach to "finite-size" particles, three challenges arise. First, the undisturbed flow seen by the particles cannot be anymore taken to be the computed carrier phase velocity at the grid scale. Although the definition of undisturbed flow as one that would exist in the absence of the particle still remains, its evaluation is computationally prohibitive, since this would require many additional simulations with one particle removed in each simulation. Second, since the undisturbed carrier phase velocity now varies over the size of the particle, its characterization in terms of only the ambient fluid velocity at the center of the particle is not sufficient. The undisturbed velocity seen by the particle requires a more complex description. Finally, even if the undisturbed flow is known and characterized to great precision, its effect on the particle in terms of force and heat transfer have not been accurately correlated for application in the point–particle context, especially at finite Re. These difficulties of course become unimportant as the particle size becomes much smaller than the smallest eddies.

Based on current understanding, the best possible approach to evaluating the force on a finite-size point–particle (whose diameter is comparable to the carrier flow scales) is to consider a deterministic contribution and a stochastic contribution. The deterministic contribution to the force on the particle will account for the effect of the carrier phase at scales much larger than the particle. For the deterministic contribution one can use, for example, the standard drag correlation, with the large scale's contribution to the carrier flow at the particle location as the fluid velocity seen by the particle. The contribution from the smaller eddies of size comparable to the particle to the force on the particle must be accounted in a different way. Since the undisturbed flow at this scale and its contribution to force are hard to establish in a deterministic fashion, it is best to represent the effect of the smaller eddies as a stochastic contribution. In other words, even if the entire range of carrier flow scales are computed directly, in case of finite-size point–particles it is convenient to filter the carrier phase into large-than-particle scales and smaller scales. The former will contribute to the deterministic force and the later to the stochastic component.

6.2. Point–particle LES

In case of LES of carrier phase, let us first consider the case of particles being an order of magnitude or more smaller than the smallest resolved scales. The point–particle LES approach is then on solid footing. The undisturbed ambient resolved-scale flow can be taken to be the LES carrier phase velocity at the particle location and its contribution to force can be estimated using the standard drag law. The unresolved subgrid scale will also influence particle motion and must be taken into account with a stochastic contribution. Stochastic Langevin type models have been developed to account for the influence of unresolved subgrid scales on particle motion (Minier et al., 2004; Shotorban and Balachandar, 2006; Berrouk et al., 2007).

If the particles under consideration are large and of comparable size to the smallest resolved eddies, then difficulties similar to those outlined for DNS of carrier phase arise. Again, it is appropriate to filter the resolved scales into substantially larger-than-particle scales and smaller resolved scales. The former will contribute to the deterministic force, while the later can be combined with the unresolved scales and accounted through the stochastic contribution.

The effect of particles on LES closure of carrier phase equations must also be considered. If the particles are much smaller than the smallest resolved scale (as depicted in Fig. 1b), then a conventional single phase LES closure with back coupling of forces from the particles can be expected to be sufficient. However, if point–particle LES approach is pushed to allow the LES cut-off length scale to fall within the range of disturbance flow due to the particles, it is not clear if and how the subgrid scale closure must be modified to account for the overlap.

The effect of particle Reynolds number must be considered as well. As can be seen from Fig. 4, in the context of DNS even for particles as large as the Kolmogorov scale their Reynolds number remains low. In the context of LES the particle Reynolds number can be much larger. In a steady uniform ambient flow for $\mathrm{Re} > 280$ the wake becomes unsteady with periodic vortex shedding and correspondingly the force acting on the particle shows periodic fluctuation. In a turbulent flow the critical Reynolds number for onset of vortex shedding decreases (Bagchi and Balachandar, 2003). At even higher Reynolds numbers the wake dynamics and the force acting on the particle become chaotic. Thus, in cases where particle Reynolds number exceed few hundred, the effect of vortex shedding on force fluctuation must also be accounted as added contribution to the stochastic component of the particle force.

Finally, the effect of particle volume fraction can be considered. So far we have assumed that particle volume fraction to be quite small. Here it must be stressed that even if mean volume fraction is quite small, due to preferential accumulation, there can be local regions where volume fraction can build up to large values. With increasing volume fraction, particle–particle interaction becomes significant and this inter-particle interaction must be taken into account in the momentum and energy exchange between phases.

7. Summary

Simple dimensional arguments are used in establishing three different regimes where relative velocity between the particle and the carrier phase are differently controlled. In regime-I particles are sufficiently small that the relative velocity is dictated by the Kolmogorov eddies. In regime-II particles are larger and their relative velocity is controlled by an inertial range eddy whose time scale matches that of the particle. In regime-III the particles are large that their time scale exceeds that of the integral scale eddies and in this regime relative velocity is dictated by the integral scale eddies. The relative velocity scaling is used to subsequently obtain estimates of particle Reynolds number and Stokes number in terms of nondimensional particle size (d/η) and density ratio.

From a comparative analysis of the different computational approaches available for turbulent multiphase flows it is argued that the point–particle approach is uniquely suited to address turbulent multiphase flows where the Stokes number, defined as the ratio of particle time scale to Kolmogorov time scale (τ_p/τ_k), is greater than 1. The point–particle approach is clearly applicable even when $\tau_p/\tau_k < 1$, however, when Stokes number is smaller than about 0.2 the equilibrium Eulerian approach offers a more computationally efficient alternative. In the limit $\tau_p/\tau_k \ll 1$ one may even simply use the dusty gas approximation. For the case $0.2 < \tau_p/\tau_k \sim O(1)$ both the Eulerian two-fluid formulation and the Lagrangian point–particle approach become comparable. In particular for larger particles of $\tau_p/\tau_k > 1$, since uniqueness of particle velocity cannot be guaranteed, Lagrangian approach offers a definite advantage over the Eulerian approaches.

The Stokes number estimate has been used to recast the above arguments and establish parameter range where point–particle approach is ideally suited. If we restrict attention to only particles of size an order of magnitude or more smaller than the smallest computed eddies, in the context of DNS of carrier phase, the point–particle approach perhaps makes sense only for very heavy particles. For lighter particles and bubbles, their Stokes number will be so low that computationally more efficient Dusty gas or equilibrium Eulerian approaches should be sufficient. In the contact of LES of carrier phase, the point–particle approach presents unique advantage over Eulerian approaches for substantially heavier-than-fluid particles and becomes comparable to the two-fluids approach in case of near-neutrally buoyant particles. If we push the applicability of the point–particle approach to larger particles of size that approach the smallest resolved eddies, then point–particle approach presents unique opportunity for a wider range of density ratio, including lighter-than-fluid bubbles. However, as we extend the point–particle approach to "finite-size" particles new challenges arise in the implementation of Lagrangian–Eulerian coupling between the particles and the carrier phase. An approach where the inter-phase momentum and energy coupling can be separated into a deterministic and a stochastic contribution has been suggested.

A. More accurate estimation relative velocity

Consider a one-dimensional oscillatory flow $u = Real\{u_0 e^{\imath\omega t}\}$. The particle motion in given by

$$\frac{dv}{dt} = \frac{u - v}{\tau_p} + \beta\frac{Du}{Dt}. \tag{20}$$

Here d/dt is total derivative following the particle and D/Dt is that following the fluid element. The resulting solution can be used to evaluate the relative velocity between the particle and the flow. In particular, if we consider the oscillatory flow to correspond to an l-size eddy with $u_0 \sim u_l$ and $\omega \sim 1/\tau_l$ the relative velocity due to the l-size eddy can be written as

$$\frac{(u-v)_l}{u_l} = (1-\beta)\frac{\tau_p/\tau_l}{[1+(\tau_p/\tau_l)^2]^{1/2}}, \tag{21}$$

which can be compared with (2) and verified that the equilibrium Eulerian approach provides an adequate approximation to the relative velocity. The above more refined estimate of the l-size eddy's effect on relative velocity can be used in a manner similar to that outlined in Section 3. Again three different regimes can be identified. Interestingly the regime boundaries remain the same as those given in (3), (6) and (7). The relative velocity in the three regimes can now be expressed as

$$-v = \begin{cases} \frac{u_k(1-\beta)(\tau_p/\tau_k)}{[1+(\tau_p/\tau_k)^2]^{1/2}} & \text{for } \tau_p < \tau_k \\ \frac{1-\beta}{\sqrt{2}} u_l(\epsilon\tau_p)^{1/2} & \text{for } \tau_k < \tau_p < \tau_L \\ \frac{(1-\beta)(\epsilon L)^{1/3}(\tau_p/\tau_L)}{[1+(\tau_p/\tau_L)^2]^{1/2}} & \text{for} \tau_L < \tau_p \end{cases} \tag{22}$$

The above expression for relative velocity can be compared with those given in (3), (6) and (7) and verified that the general scaling arguments presented here are robust.

Acknowledgments

This research was supported by NSF CBET0639446 and NSF EAR0609712.

References

Bagchi, P., Balachandar, S., 2003. Effect of turbulence on the drag and lift of a particle. Phys. Fluids 15, 3496–3513.
Bagchi, P., Balachandar, S., 2004. Response of the wake of an isolated particle to an isotropic turbulent flow. J. Fluid Mech. 518, 95–123.
Balachandar, S., 2003. Parameterization of force on a particle/bubble/droplet. Multiphase Sci. Tech. 15, 157–171.
Berrouk, A.S., Laurence, D., Riley, J.J., Stock, D.E., 2007. Stochastic modeling of inertial particle dispersion by subgrid motion for LES of high Reynolds number pipe flow. J. Turbulence 8, N50.
Burton, T.M., Eaton, J.K., 2005. Fully resolved simulations of particle–turbulence interaction. J. Fluid Mech. 545, 67–111.
Clift, R., Grace, J.R., Weber, M.E., 1978. Bubbles, Drops and Particles. Academic, New York.
Druzhinin, O.A., Elghobashi, S., 1999. On the decay rate of isotropic turbulence laden with microparticles. Phys. Fluids 11, 602–610.
Elghobashi, S., 1991. Particle-laden turbulent flows: direct simulation and closure models. Appl. Sci. Res. 48, 301–314.
Elghobashi, S., Truesdell, G.C., 1992. Direct simulation of particle dispersion in a decaying isotropic turbulence. J. Fluid Mech. 242, 655–700.
Elghobashi, S., Truesdell, G.C., 1993. On the 2-way interaction between homogeneous turbulence and dispersed solid particles 1. Turbulence modification. Phys. Fluids A 5, 1790–1801.
Elghobashi, S., 1994. On predicting particle-laden turbulent flows. Appl. Sci. Res. 52, 309–329.
Ferrante, A., Elghobashi, S., 2004. On the physical mechanism of drag reduction in a spatially developing turbulent boundary layer laden with microbubbles. J. Fluid Mech. 503, 345–355.
Ferry, J., Balachandar, S., 2001. A fast Eulerian method for two-phase flow. Int. J. Multiphase Flow 27, 1199–1226.
Ferry, J., Rani, S.L., Balachandar, S., 2003. A locally implicit improvements of the equilibrium Eulerian method. Int. J. Multiphase Flow 29, 869–891.
Ferry, J., Balachandar, S., 2002. Equilibrium expansion for the Eulerian velocity of small particles. Powder Technol. 125, 131–139.
Ferry, J., Balachandar, S., 2005. Equilibrium Eulerian approach for predicting the thermal field of a dispersion of small particles. Int. J. Heat Mass Transfer 48, 681–689.
Fevrier, P., Simonin, O., Squires, K.D., 2005. Partitioning of particle velocities in gas–solid turbulent flows into a continuous field and a spatially uncorrelated random distribution: theoretical formalism and numerical study. J. Fluid Mech. 533, 1–46.
Fox, R.O., Laurent, F., Massot, F., 2008. Numerical simulation of spray coalescence in an Eulerian framework: direct quadrature method of moments and multi-fluid method. J. Comput. Phys. 277, 3058–3088.
Kajishima, T., Takiguchi, S., Hamasaki, H., Miyake, Y., 2001. Turbulence structure of particle-laden flow in a vertical plane channel due to vortex shedding. JSME Int. J. Ser. B – Fluids Thermal Eng. 44, 526–535.
Kallio, G.A., Reeks, M.W., 1989. A numerical simulation of particle deposition in turbulent boundary layers. Int. J. Multiphase Flow 15, 433–446.
Lu, J.C., Tryggvason, G., 2006. Numerical study of turbulent bubbly downflows in a vertical channel. Phys. Fluids 18, 103302.
Marble, F.E., 1970. Dynamics of dusty gases. Ann. Rev. Fluid Mech. 2, 397–446.
Maxey, M.R., 1987. The gravitational settling of aerosol particles in homogeneous turbulence and random flow fields. J. Fluid Mech. 174, 441–465.
McGraw, R., 1997. Description of aerosol dynamics by the quadrature method of moments. Aerosol. Sci. Technol. 27, 255–265.
McLaughlin, J.B., 1989. Aerosol particle deposition in numerically simulated channel flow. Phys. Fluids A 1, 1211–1224.
Mei, R., 1994. Effect of turbulence on the particle settling velocity in the nonlinear drag range. Int. J. Mulitphase Flow 20, 273–284.
Merle, A., Legendre, D., Magnaudet, J., 2005. Forces on a high-Reynolds-number spherical bubble in a turbulent flow. J. Fluid Mech. 532, 53–62.
Minier, J.P., Peirano, E., Chibbaro, S., 2004. PDF model based on Langevin equation for polydispersed two-phase flows applied to bluff-body gas–solid flows. Phys. Fluids 16, 2419–2431.

Pan, Y., Banerjee, S., 1997. Numerical investigation of the effects of large particles on wall turbulence. Phys. Fluids 9, 3786–3807.
Pope, S.B., 1985. PDF methods for turbulent reactive flows. Prog. Energy Combust. Sci. 11, 119–192.
Rani, S.L., Balachandar, S., 2003. Evaluation of the equilibrium Eulerian approach for the evolution of particle concentration in isotropic turbulence. Int. J. Multiphase Flow 29, 1793–1816.
Reeks, M.W., 1983. The transport of discrete particles in inhomogeneous turbulence. J. Aerosol Sci. 14, 729–739.
Riley, J.J., Paterson, G.S., 1974. Diffusion experiments with numerically integrated isotropic turbulence. Phys. Fluids 17, 292–297.
Saffman, P.G., 1962. On the stability of laminar flow of a dusty gas. J. Fluid Mech. 13, 120–128.
Shotorban, B., Mashayek, F., 2006. A stochastic model for particle motion in large-eddy simulation. J. Turbulence 7 (18).
Shotorban, B., Balachandar, S., 2006. Particle concentration in homogeneous shear turbulence simulated vis Lagrangian and equilibrium Eulerian approaches. Phys. Fluids 18, 065105.
Squires, K.D., Eaton, J., 1991. Preferential concentration of particles by turbulence. Phys. Fluids A 3, 1169–1179.
Subramaniam, S., 2001. Statistical modeling of sprays using the droplet distribution function. Phys. Fluids 13, 624–642.
Sundaram, S., Collins, L.R., 1997. Collision statistics in an isotropic particle-laden turbulent suspension 1. Direct numerical simulations. J. Fluid Mech. 335, 75–109.
Ten Cate, A., Derksen, J.J., Portela, L.M., Van den Akker, H., 2004. Fully resolved simulations of colliding monodisperse spheres in forced isotropic turbulence. J. Fluid Mech. 519, 233–271.
Uhlmann, 2008. Interface-resolved direct numerical simulation of vertical particulate channel flow in the turbulent regime. Phys. Fluids, 053305.
Wang, L.P., Maxey, M.R., 1993. Settling velocity and concentration distribution of heavy particles in homogeneous isotropic turbulence. J. Fluid Mech. 256, 27–68.
Wang, Q., Squires, K.D., 1997. Large eddy simulation of particle-laden turbulent channel flow. Phys. Fluids 8, 1207–1223.
Yamamoto, Y., Potthoff, M., Tanaka, T., Kajishima, T., Tsuji, Y., 2001. Large eddy simulation of turbulent gas–particle flow in a vertical channel: effect of considering interparticle collisions. J. Fluid Mech. 442, 303–334.
Zeng, L., Balachandar, S., Fischer, P., Najjar, F.M., 2008. Interactions of a stationary finite-sized particle with wall turbulence. J. Fluid Mech. 594, 271–305.